

Prediction of Added Resistance by Means of Unsteady Wave-Pattern Analysis

Masashi Kashiwagi

Department of Naval Architecture & Ocean Engineering, Osaka University
2-1 Yamada-oka, Suita, Osaka 565-0871, Japan, E-mail: *kashi@naoe.eng.osaka-u.ac.jp*

1. Introduction

The added resistance in waves is crucial in predicting the speed loss of a ship navigating in actual seas. Thus a large number of work has been made so far. However, details in the hydrodynamic relation between the added resistance and the wave amplitude function seem to be unclear, because the added resistance is an integrated quantity of the pressure and comparisons have been made between this integrated value and the total increase in the ship resistance in waves measured by a dynamometer.

Ohkusu (1980) proposed a method for measuring ship-generated unsteady waves and then evaluating the wave amplitude function and the added resistance. This analysis method enables a comparison at the level of wave profile and thus may provide us with deeper hydrodynamic understanding. However, accurate measurement of unsteady waves is not so easy and subsequent analyses for the Fourier transform of wave elevation and for the added resistance have not been made in a convincing manner.

In the present study, in addition to direct measurement of the added resistance by a dynamometer, ship-generated unsteady waves are measured. Numerical computations corresponding to the experiment are performed with enhanced unified theory (EUT) developed by Kashiwagi (1995). Then a comparison is made for the wave profile along a longitudinal line parallel to the ship's advancing direction. Not only measured waves but also computed ones are used to validate the wave analysis method for predicting the added resistance and to study the effects of local wave and lateral distance for the wave measurement. Discussion is also made on which part of the wave is crucial and hence where attention should be paid in predicting the added resistance from the wave-pattern analysis.

2. Unsteady Wave Analysis and Added Resistance

Let us consider a ship advancing at constant forward speed U into a regular wave of amplitude A , circular frequency ω_0 . The depth of water is assumed infinite and thus the wavenumber of incident wave is given by $k_0 = \omega_0^2/g$, with g the gravitational acceleration. For brevity, only the head wave is considered, and the analysis is made with a right-hand Cartesian coordinate system $Oxyz$, with the origin placed at the center of a ship and on the undisturbed free surface, which translates with the same constant speed as that of the ship along the positive x -axis. The z -axis is positive downward. Unsteady ship responses and ambient unsteady flow of fluid are assumed to be linear and periodical with circular frequency of encounter $\omega = \omega_0 + k_0 U$.

Assuming the flow inviscid with irrotational motion, the velocity potential is introduced and written in the form

$$\Phi(x, y, z, t) = -Ux + \text{Re} \left[\left\{ \phi_0(x, y, z) + \phi(x, y, z) \right\} e^{i\omega t} \right], \quad (1)$$

where ϕ_0 denotes the incident-wave potential and ϕ the disturbance potential. By linear assumption, the disturbance potential is decomposed in the form

$$\phi(x, y, z) = \frac{gA}{i\omega_0} \left\{ \phi_7(x, y, z) - \frac{\omega\omega_0}{g} \sum_{j=1,3,5} \frac{X_j}{A} \phi_j(x, y, z) \right\}. \quad (2)$$

Here ϕ_7 denotes the scattering potential and ϕ_j the radiation potential due to the j -th mode of motion ($j = 1, 3, 5$ for surge, heave, and pitch, respectively) with X_j its complex amplitude.

The elevation of ship-generated wave in the linear theory can be computed by

$$\zeta_w(x, y) = \frac{1}{g} \left(i\omega - U \frac{\partial}{\partial x} \right) \phi(x, y, 0) \quad (3)$$

and each component in the disturbance potential is evaluated in the present paper by the far-field representation in the slender-ship theory as follows:

$$\phi_j(x, y, 0) = \int_L Q_j(\xi) G(x - \xi, y, 0) d\xi \quad (j = 1, 3, 5, 7), \quad (4)$$

where $Q_j(x)$ denotes the strength of sources distributed along the x -axis and $G(x, y, z)$ the Green function, equivalent to the velocity potential due to an oscillating and translating source with unit strength. By substituting (2) and (4) into (3) and expressing $\zeta_W(x, y)$ as $A\zeta(x, y)$, the wave elevation normalized with incident-wave amplitude can be computed from

$$\begin{aligned} \zeta(x, y) = & -\frac{1}{2\pi^2} \int_{-\infty}^{\infty} dk \int_0^{\infty} \tilde{C}(k) e^{-ikx - |y|\sqrt{n^2 + k^2}} \frac{n^2 dn}{(n^2 + \kappa^2)\sqrt{n^2 + k^2}} \\ & - \frac{1}{2\pi} \left[\int_{k_1}^{k_2} + \int_{k_3}^{k_4} \right] \tilde{C}(k) \frac{\kappa}{\sqrt{k^2 - \kappa^2}} e^{-ikx - |y|\sqrt{k^2 - \kappa^2}} dk \\ & + \frac{i}{2\pi} \left[-\int_{-\infty}^{k_1} + \int_{k_2}^{k_3} + \int_{k_4}^{\infty} \right] \tilde{C}(k) \frac{\kappa}{\sqrt{\kappa^2 - k^2}} e^{-ikx - i\epsilon_k |y|\sqrt{\kappa^2 - k^2}} dk, \end{aligned} \quad (5)$$

where

$$\left. \begin{aligned} \kappa &= \frac{1}{g} (\omega + kU)^2 = K + 2k\tau + \frac{k^2}{K_0}, \\ K &= \frac{\omega^2}{g}, \quad \tau = \frac{U\omega}{g}, \quad K_0 = \frac{g}{U^2}, \quad \epsilon_k = \text{sgn}(\omega + kU), \end{aligned} \right\} \quad (6)$$

$$\left. \begin{aligned} k_1 \} &= -\frac{K_0}{2} (1 + 2\tau \pm \sqrt{1 + 4\tau}), & k_3 \} &= \frac{K_0}{2} (1 - 2\tau \mp \sqrt{1 - 4\tau}), \\ k_2 \} & & k_4 \} & \end{aligned} \right\} \quad (7)$$

$$\tilde{C}(k) = \frac{(\omega + kU)}{\omega_0} C(k), \quad C(k) = C_7(k) - \frac{\omega\omega_0}{g} \sum_{j=1,3,5} \frac{X_j}{A} C_j(k), \quad (8)$$

$$C_j(k) = \int_L Q_j(\xi) e^{ik\xi} d\xi. \quad (9)$$

Here $C_j(k)$ is defined as the Kochin function of each component in the disturbance potential and $C(k)$ in (8) is the total Kochin function for the case of all modes of motion free to oscillate in a wave.

The first and second lines on the right-hand side of (5) represent local waves. Neglecting these, (5) can be expressed in the form

$$\zeta(x, y) \simeq \frac{i}{2\pi} \int_{-\infty}^{\infty} u(\kappa^2 - k^2) C(k) \sqrt{\frac{\kappa}{k_0}} \frac{\kappa}{\sqrt{\kappa^2 - k^2}} e^{-ikx - i\epsilon_k |y|\sqrt{\kappa^2 - k^2}} dk, \quad (10)$$

where $u(\kappa^2 - k^2)$ is the unit step function, equal to 1 for $\kappa^2 > k^2$ and zero otherwise. It should also be noted that $\epsilon_k = \text{sgn}(\omega + kU) = -1$ for $-\infty < k < k_1$ and $\epsilon_k = 1$ for $k_2 < k < \infty$.

Let us consider the Fourier transform of $\zeta(x, y)$ with respect to x , defined by the following integral:

$$\zeta^*(\ell, y) = \int_{-\infty}^{\infty} \zeta(x, y) e^{i\ell x} dx. \quad (11)$$

Mathematically, in terms of an integral representation of Dirac's delta function

$$\frac{1}{2\pi} \int_{-\infty}^{\infty} e^{i(\ell - k)x} dx = \delta(\ell - k), \quad (12)$$

the following relation can readily be obtained:

$$\zeta^*(k, y) = i C(k) \sqrt{\frac{\kappa}{k_0}} \frac{\kappa}{\sqrt{\kappa^2 - k^2}} e^{-i\epsilon_k |y|\sqrt{\kappa^2 - k^2}}. \quad (13)$$

Namely the Fourier transform of the wave elevation is directly connected with the Kochin function as in (13).

According to Maruo's theory for the added resistance, the added resistance in head waves can be computed in terms of the Kochin function as follows:

$$\begin{aligned} \frac{R_{AW}}{\rho g A^2} &= \frac{1}{4\pi k_0} \left[-\int_{-\infty}^{k_1} + \int_{k_2}^{k_3} + \int_{k_4}^{\infty} \right] |C(k)|^2 \frac{\kappa}{\sqrt{\kappa^2 - k^2}} (k + k_0) dk \\ &= \frac{1}{4\pi k_0} \int_{-\infty}^{\infty} \epsilon_k u(\kappa^2 - k^2) |C(k)|^2 \frac{\kappa}{\sqrt{\kappa^2 - k^2}} (k + k_0) dk. \end{aligned} \quad (14)$$

Thus, substituting (13) in (14) provides a formula for computing the added resistance with the Fourier transform of ship-generated unsteady waves, in the form

$$\frac{R_{AW}}{\rho g A^2} = \frac{1}{4\pi} \left[-\int_{-\infty}^{k_1} + \int_{k_2}^{k_3} + \int_{k_4}^{\infty} \right] |\zeta^*(k, y)|^2 \frac{\sqrt{\kappa^2 - k^2}}{\kappa^2} (k + k_0) dk. \quad (15)$$

3. Numerical Computations and Experiment

Experiments were carried out in head waves, measuring the wave-induced motions (surge, heave, and pitch), the added resistance by a dynamometer, and also ship-generated unsteady waves using six wave probes of capacitance type which are positioned with almost equal intervals over one period of encounter. The spatial distribution of cosine and sine components in the unsteady wave oscillating with circular frequency of encounter ω were obtained by the least-squares method using the data measured with six wave probes along a longitudinal line parallel to the x -axis (at constant y).

The ship model used in the experiments and also numerical computations is a modified Wigley model with wider breadth, expressed mathematically as

$$\left. \begin{aligned} \eta &= (1 - \zeta^2)(1 - \xi^2)(1 + 0.6\xi^2 + \xi^4) + \zeta^2(1 - \zeta^8)(1 - \xi^2)^4 \\ \xi &= \frac{2x}{L}, \quad \eta = \frac{2y}{B}, \quad \zeta = \frac{z}{d} \end{aligned} \right\} \quad (16)$$

where the real dimensions are $L = 2.5$ m, $B = 0.5$ m, $d = 0.175$ m (which is called standard draft). The gyration radius in pitch and the center of gravity were set to $\kappa_{yy}/L = 0.236$ and $\overline{OG}/d = 0.177$ (below the free surface).

The lateral distance of a longitudinal line used for the wave measurement from the centerline of a ship model (i.e. x -axis) was set equal to $y = B/2 + 0.1\text{m} = 0.35$ m. The Froude number was $Fn = 0.2$ in all measurements.

Numerical computations corresponding to the experiments were performed by means of the enhanced unified theory (EUT) developed by Kashiwagi (1995). This theory can compute the surge-related quantities with 3-D and forward-speed effects taken into account and also the effect of wave diffraction near the bow by retaining the contribution of the x -component of the normal vector in the body boundary condition. In EUT, the radiation and diffraction problems are solved, with 3-D and forward-speed effects incorporated through a homogeneous component in the inner solution, and those effects are reflected through the matching procedure into the source distribution $Q_j(x)$ in the outer solution and then the Kochin function to be computed from (8) and (9). Of course the complex amplitude X_j was determined by solving the equations of ship motion.

4. Results and Discussion

Figure 1 shows a comparison of the added resistance, in which open circles show the results measured by a dynamometer and the solid line shows computed results by EUT in terms of the Kochin function and Maruo's formula (14). Closed triangles indicate the results obtained from the wave-pattern analysis (15), using the measured data over the range of $3 > x/(L/2) > -5$ and no correction is made for the downstream wave profile. One example of the measured wave elevation is shown in Fig. 2 which is for $\lambda/L = 1.0$, and the cosine and sine components correspond to the coefficients in the Fourier-series expansion and thus they can be expressed as $\zeta(x, y) = \zeta_C(x, y) - i\zeta_S(x, y)$ in complex notation.

In order to compare this wave profile with computed one and to understand effects of the local wave and lateral distance in the wave measurement and which part of the wave is dominant in the prediction of the added resistance, numerical computations of the wave elevation and added resistance were performed using EUT. It should be noted that the position of the source distribution in EUT is, as shown by (4) or (9), just on the free surface ($z_s = 0$) and along the x -axis ($y_s = 0$). In this case, as shown in Fig. 3, the shorter-wavelength component becomes conspicuous, which looks much different from the measured one. However, it is confirmed that the added resistance computed from the Fourier transform of this computed wave profile is in virtually perfect agreement with the solid line shown in Fig. 1. (It is noteworthy that the wave measurement has been done only with six wave probes, which may not be enough for resolving shorter waves.)

Anyhow, to suppress the amplitude of shorter-wave component, the depth-wise position of the source distribution is slightly shifted with $z_s = 0.004d$ (0.4% of draft). This slight shift affects greatly the result of the wave profile, resembling the measured one. However, the resulting added resistance computed from (15) becomes much smaller than the value by the original EUT.

Thus the entire wave profile is 1.75 times magnified and shown as Fig. 4. With this magnification in the amplitude, the added resistance becomes almost the same as that to be computed from Fig. 3.

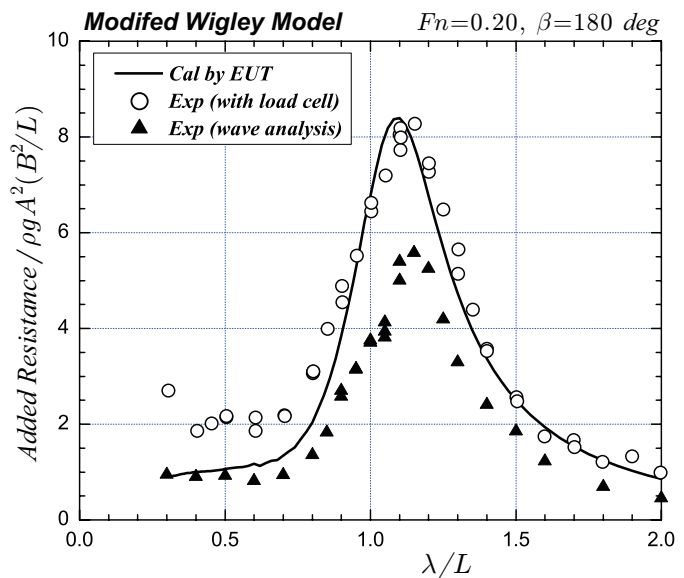


Fig. 1 Comparison of the added resistance on modified Wigley model in head waves at $Fn = 0.2$.

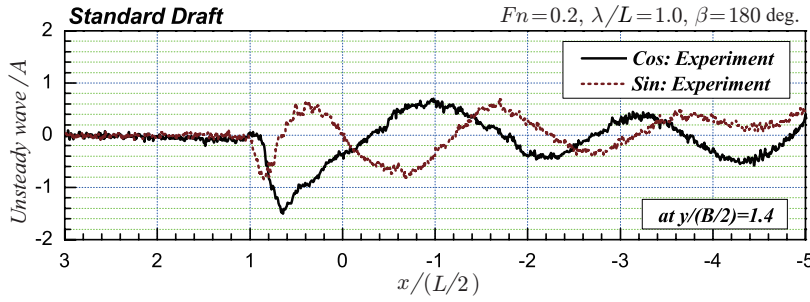


Fig. 2 Unsteady wave generated by modified Wigley model, measured by wave probes positioned at $y/(B/2) = 1.4$, for head wave of $\lambda/L = 1.0$ at $Fn = 0.2$.

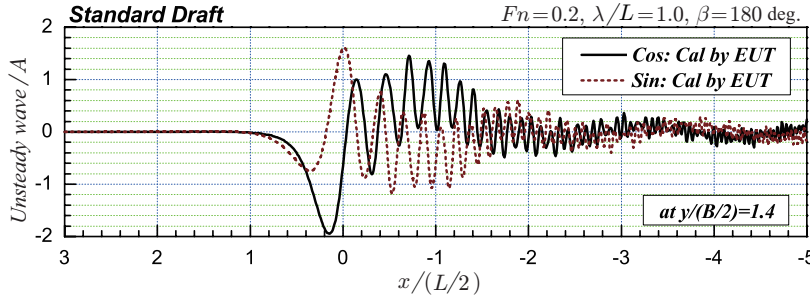


Fig. 3 Unsteady wave generated by modified Wigley model, computed with EUT at $y/(B/2) = 1.4$, for head wave of $\lambda/L = 1.0$ and $Fn = 0.2$. The source distribution is placed at $z_s = 0.0$.

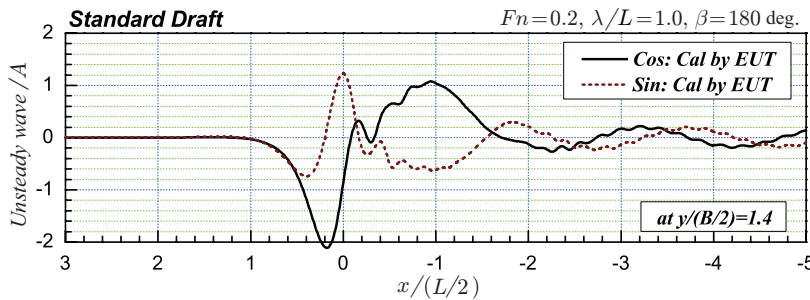


Fig. 4 Unsteady wave generated by modified Wigley model, computed with EUT at $y/(B/2) = 1.4$, for head wave of $\lambda/L = 1.0$ and $Fn = 0.2$. The source distribution is placed at $z_s/d = 0.004$ and the amplitude is 1.75 times magnified.

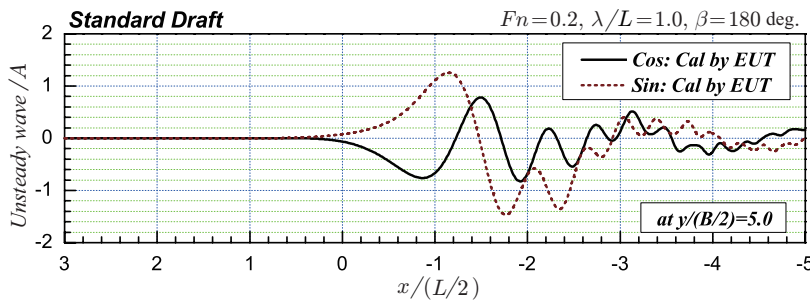


Fig. 5 Unsteady wave generated by modified Wigley model, computed with EUT at $y/(B/2) = 5.0$ ($y/(L/2) = 1.0$), for head wave of $\lambda/L = 1.0$ and $Fn = 0.2$. The source distribution is placed at $z_s/d = 0.004$ and the amplitude is 1.75 times magnified.

References

- 1) Ohkusu, M. 1980: Added Resistance in Waves in the Light of Unsteady Wave Pattern Analysis, *Proc. of 13th Symp. on Naval Hydrodynamics*, Tokyo, pp. 413–425.
- 2) Kashiwagi, M. 1995: Prediction of Surge and Its Effect on Added Resistance by Means of the Enhanced Unified Theory, *Trans. West-Japan Society of Naval Architects*, No. 89, pp. 77–89.

By comparison between Fig. 2 (measurement) and Fig. 4 (computation), prominent discrepancy can be seen in the range of $1 > x/(L/2) > 0$. In EUT, the far-field disturbance by a ship is represented by the source distribution along the x -axis, whereas in the experiment, the half breadth of ship model is $B/2 = 0.25$ m and thus the so-called displacement effect becomes obvious (the wave pattern tends to be shifted to transversely outward direction).

Through the present numerical study on the analysis of wave profile and resultant added resistance, following facts have been found:

[1] The amplitude (profile) of the wave generated near the bow and propagating ahead is dominant in the added resistance. In the examples shown as Fig. 2 – Fig. 4, the waves at $|x/(L/2)| < 1$ are especially important and little influence exists from the downstream waves. This implies that the prediction of the added resistance from the measured wave elevation can be successfully made without any correction for the downstream waves (which actually cannot be measured due to reflection from side walls of a towing tank).

[2] The effect of local wave is very small and negligible in the added resistance. In fact, the added resistance was virtually the same irrespective of whether the local wave components in (5) are included in the numerical computation by EUT.

[3] The effect of lateral position in the wave measurement is also very small. In fact, the wave profile was computed also at $y = L/2 = 1.25$ m (the result of which is shown as Fig. 5) and the added resistance computed from this wave profile was virtually the same as that computed from the wave profile at $y = 0.35$ m shown in Fig. 4.

From the consideration above, relations between the added resistance and the unsteady wave analysis were elucidated. Consequently it can be understood that careful attention must be paid in measuring the waves (including short-wave component) generated from the bow part of a ship, because slight error in the wave amplitude may result in large difference in the added resistance.